PROCEEDINGS OF SCIENCE

News from BESIII

Stephen Lars Olsen
Department of Physics & Astronomy, Seoul National University
Gwanak-gu, Seoul, 151-747, KOREA
E-mail: solsen@hep1.snu.ac.kr

Representing the BESIII Collaboration

BESIII is a new state-of-the-art 4π detector at the recently upgraded BEPCII two-ring e^+e^- collider at the Institute of High Energy Physics in Beijing. It has been in operation for three years, during which time it has collected the world's largest data samples of J/ψ, ψ' and $\psi(3770)$ decays. These data are being used to make a variety of interesting and unique studies of light-hadron spectroscopy, precision charmonium physics and high-statistics measurements of D meson decays. Results that I describe in this report include studies of $a_0(980)$-$f_0(980)$ mixing, an observation of a large isospin-violation in $\eta(1405) \to \pi^0 f_0(980)$ decays, some puzzles in J/ψ and ψ' decays to light hadrons, the observation of two glueball candidate states in radiative $J/\psi \to \gamma\pi^+\pi^-\eta'$ decays and some recent precision measurements of η_c and h_c lineshapes.

50th International Winter Meeting on Nuclear Physics - Bormio2012,
23-27 January 2012
Bormio, Italy

PoS(Bormio2012)021

1. Introduction

The BES experimental program dates back to late 1989 when operation of the Beijing Electron Positron Collider (BEPC) and the Beijing Electron Spectrometer (BES) first started. BEPC was a single-ring e^+e^- collider that operated in the τ-charm threshold energy region between (about) 2.5 and 4.5 GeV with a luminosity of $\sim 10^{31}\text{cm}^{-2}\text{s}^{-1}$. Among the early successes included a precise measurement of the mass of the τ lepton [1] that not only improved on the precision of previous measurements by an order-of-magnitude, but also showed that the existing world avearge value was high by about two standard deviations. Another key result was the precise measurement of the total cross section for e^+e^- annihilation into hadrons over the accessible center of mass (c.m.) energy range [2]. The precision of these measurements lead to a substantially improved evaulation of the electromagnetic coupling constant extrapolated to the Z-boson mass peak, $\alpha_{QED}(M_Z^2)$, which resulted in a significant $\sim$30% increase in the Standard Model (SM) predicted value for the Higgs' boson mass [3].

In the late 1990s, the BES detector was upgraded to the BESII detector and this produced a number of interesting results including even more precise cross section measurements [4] and the discovery of a number of new hadron states, including the σ [6] and κ [5] scalar resonances and a still-unexplained subthreshold $p\bar{p}$ resonance produced in radiative $J/\psi \to \gamma p\bar{p}$ decays [7].

Between 2005 and 2008, BEPC was replaced by BEPCII, a two-ring e^+e^- collider with a hundred-fold increase in luminosity, and the BESII detector was completely removed and replaced by BESIII, a state-of-the-art detector built around a 1 T superconducting solenoid that contains a cylindrical drift chamber, a double-layer barrel of scintillation counters for time-of-flight measurements, and a nearly 4π array of 6240 CsI(Tl) crystals for electromagnetic calorimetry. The magnet's iron flux-return yoke is instrumented with a nine-layer RPC muon identification system. BEPCII operations started in summer 2008 and since then the luminosity has been continuously improving; now it is $\sim 6\times 10^{32}\text{cm}^{-2}\text{s}^{-1}$, quite near the 10^{33} design value. The BESIII detector performance is excellent: the charged particle momentum resolution is $\delta p/p \simeq 0.5\%$; the γ energy resolution is 2.5% at $E_\gamma = 1$ GeV; the 6% resolution dE/dx measurements in the drift chamber plus the $\sim$80 ps resolution time-of-flight measurements is sufficient to identify charged particles over the entire momentum range of interest.

The BESIII experimental program addresses issues in light hadron physics, charmonium spectroscopy and decays, D and D_s meson decays, and numerous topics in QCD and τ-lepton physics. To date, BESIII has accumulated data samples corresponding to 225M J/ψ decays, 106M ψ' decays and 2.9 fb^{-1} at the peak of the $\psi(3770)$ resonance, which decays to $D\bar{D}$ meson pairs nearly 100% of the time. These are all world's-largest data samples at these c.m. energies and the J/ψ sample is the first ever to be collected in a high quality detector like BESIII. In this talk I review some recent results on hadron physics that have been generated from these data samples.

2. Some issues in light hadron physics

In the original quark model, first proposed by Gell-Mann [8] and Zweig [9] in 1964, mesons are comprised of quark-antiquark ($q\bar{q}$) pairs and baryons are three-quark (qqq) triplets, a picture that accurately classified the properties of all of the hadronic particles and resonances known at

the time. Its phenomenal success at predicting virtually all of the detailed properties of the $c\bar{c}$ charmonium and $b\bar{b}$ bottomonium states that were subsequently discovered in the 1970's led to the near unanimous agreement that, in spite of the fact that an individual quark had never been seen, quarks are real objects and the quark-antiquark mesons and quark-quark-quark baryons are the basic combinations that form hadrons.

In the 1970's, this simple quark model was superseded by Quantum Chromodynamics (QCD), which identified the underlying reason for these rules was that $q\bar{q}$ pair and qqq triplet combinations are color-singlet representations of the color $SU(3)$ group that is fundamental to the theory. Somewhat suprisingly, the mesons-are-$q\bar{q}$ and baryons-are-qqq prescriptions still adequately describe the hadronic particle spectrum despite the existence of a number of other color-singlet quark and gluon combinations that are possible in QCD. These additional combinations include five-quark ($qqqq\bar{q}$) "pentaquark" baryons, four-quark ($q\bar{q}q\bar{q}$) tetraquark mesons, and mesons formed from valence gluons: either $q\bar{q}$-g hybrid mesons or g-g glueballs. However, considerable experimental efforts at searching for color singlet $qqq\bar{q}q$ pentaquark baryons have still not established any unambiguous candidate for five-quark states [10], and, although a few candidates for non-$q\bar{q}$ light-hadron meson resonances have been reported [11], none have been generally accepted as established by the hadron physics community [12].

A consequence of the $q\bar{q}$ mesons and qqq baryon rules are that light mesons[1] all come in flavor-$SU(3)$ nonets and baryons come in either nonets and decuplets. In any given multiplet, all of the particles would have the same mass in the limit where the u, d and s quark masses are equal. However, since the s-quark is in fact substantially more massive than its u and d counterparts, this symmetry is broken, and particles containing s quarks are heavier than their non-strange multiplet partners. This is illustrated in Fig. 1, where the left panel indicates the quark content of the mesons and the right panel shows the meson mass hierarchy. The isospin triplet pions have no $s\bar{s}$ content and are the lightest. The η and η' mesons are $u\bar{u}\,d\bar{d}\,s\bar{s}$ mixtures:

$$\eta = \cos\phi_P \frac{|u\bar{u}> + |d\bar{d}>}{\sqrt{2}} - \sin\phi_P |s\bar{s}> \tag{2.1}$$

$$\eta' = \sin\phi_P \frac{|u\bar{u}> + |d\bar{d}>}{\sqrt{2}} + \cos\phi_P |s\bar{s}>, \tag{2.2}$$

where $\phi_P \simeq 38^\circ$ [13]. With this mixing angle, the $s\bar{s}$ component accounts for about 35% of the η's wave function and about 46% of the η''s wave function [14]; this large $s\bar{s}$ content of the η and η' is reflected in their relatively high masses. Similar hierarchy patterns are seen for other meson nonets and also in the baryon nonet and decuplet.

2.1 The light scalar meson nonet

In spite of the quark model's great acclaim, it has always had considerable difficulty accounting for the light-mass scalar mesons, especially the $a_0^{+,-,0}(980)$ isospin triplet of mesons with $m \simeq 980$ MeV,[2] $\Gamma \simeq 100$ MeV and $J^P = 0^+$, seen in $\pi\eta$ spectra produced in two-photon collisions and $p\bar{p}$ annihilations [15], and the $f_0(980)$, its isospin-singlet counterpart, which has $J^{PC} = 0^{++}$,

[1] *i.e.*, mesons formed from only u, d & s quarks.

[2] This report uses units with $c = 1$.

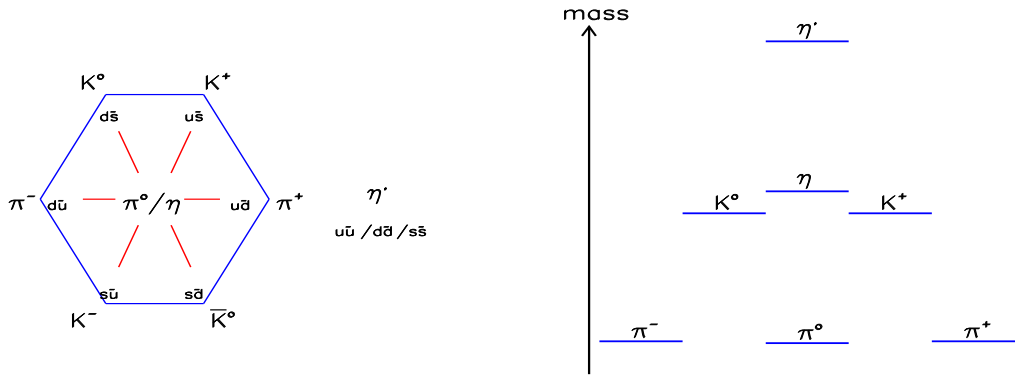

Figure 1: Left: The pseudoscalar meson nonet. The π^0 meson is a $(u\bar{u}-d\bar{d})/\sqrt{2}$ and the η and η' mesons are $u\bar{u}\,d\bar{d}\,s\bar{s}$ mixtures described in the text. **Right:** the pseudoscalar meson mass hierarchy.

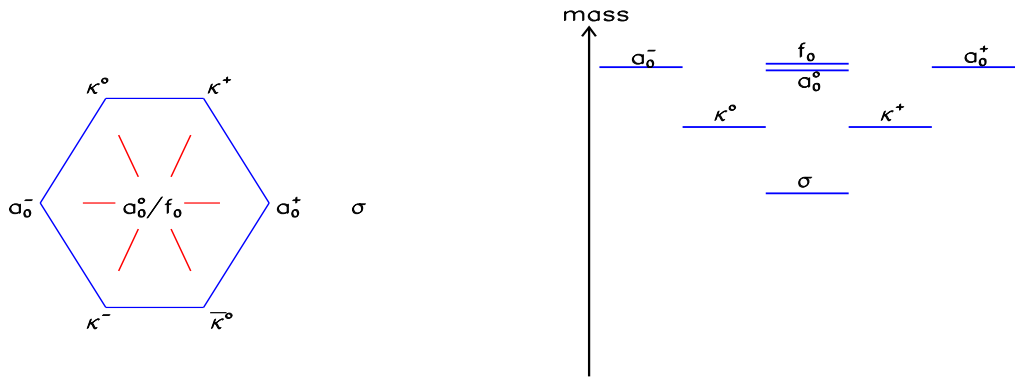

Figure 2: Left: the light scalar meson nonet. **Right:** the pseudoscalar meson mass hierarchy.

a similar mass & width, and is seen via its $f_0(980) \to \pi^+\pi^-$ decay mode in many experiments. If these are associated with the very broad, but now pretty well established $\kappa^{+,0}$ and σ^0 resonances,[3] we can identify what is called the light scalar nonet shown in the left panel of Fig. 2.

For this nonet the meson mass hierarchy, shown in the right panel of Fig. 2, is inverted; the $a_0(980)$ triplet, which in the quark model does not have any s-quark content, has the highest mass. In addition, since the $f_0(980)$ is nearly degenerate with the $a_0(980)$, the $f_0(980)$-σ mixing angle ϕ_S (the counterpart of ϕ_P in Eq. 2.2) should be nearly zero and, thus, the $f_0(980)$ should have very small s-quark content. Moreover, the higher mass tails of both the $f_0(980)$ and the $a_0(980)$ peaks are seen to have strong couplings to $K\bar{K}$ final states: a BESII study of $f_0(980)$ production in $J/\psi \to \phi\pi^+\pi^-$ and ϕK^+K^- determines the ratio of K^+K^- to $\pi^+\pi^-$ couplings of $g^{f_0}_{KK}/g^{f_0}_{\pi\pi} = 4.2 \pm 0.3$ [16] and an $a_0(980)^\pm \to K_L K^\pm$ signal seen in $p\bar{p} \to K_L K^\pm \pi^\mp$ in the Crystal Barrel experiment is used to infer $g^{a_0}_{KK}/g^{a_0}_{\eta\pi} = 1.03 \pm 0.14$ [17]. The high masses and strong couplings to K mesons suggest

[3] These are referred to as the $K^*_0(800)$ and $f_0(600)$ in the PDG tables.

Figure 3: The primary diagram for $a_0(980)$-$f_0(980)$ mixing [20].

that the $a_0(980)$ and $f_0(980)$ have substantial *s*-quark content, which is not possible in the simple $q\bar{q}$ picture for these mesons.

Another problem with a $q\bar{q}$ characterization of the light scalar-meson nonet is that the $q\bar{q}$ pair has to be in a relative *P*-wave, in which case there should be other *P*-wave nonets with $J^{PC} = 1^{+-}$, 1^{++} and 2^{++} nearby in mass. The lowest mass nonets with these quantum numbers have masses around 1300∼1500 MeV and are generally associated with a well established 0^{++} nonet in this mass region.

If the $a_0(980)$ and $f_0(980)$ are not $q\bar{q}$ states, what are they? In a classic 1977 paper, Jaffe suggested that these states might be tightly bound tetraquark states [18]. This was based on the realization that two colored quarks inside a hadron are most strongly attracted if they are in a anti-triplet in color space. This anti-color-triplet "diquark" can combine with two anticolored antiquarks in a corresponding color-triplet combination –a "diantiquark"– to form a tightly bound color-singlet diquark-diantiquark mesonic state. A different possibility, suggested by Weinstein and Isgur and motivated by the proximity of the a_0 and f_0 masses to the $K\bar{K}$ mass threshold, is that they are loosely bound molecule-like configurations of K and $\bar{K}$ mesons [19].

2.2 $a_0(980)$-$f_0(980)$ mixing?

Hanhart and collaborators [20] have suggested that the isopsin-violating $a_0(980) \leftrightarrow f_0(980)$ process would be a useful probe of the internal structure of the $a_0(980)$-$f_0(980)$ meson system. The leading diagram for mixing of this type is the difference between the K^+K^- and $K^0\bar{K}^0$ loop processes shown in Fig. 3. For $a_0(980)$) (or $f_0(980)$) mass values that are either below $2m_{K^+}$ or above $2m_{K^0}$, the two diagrams more-or-less cancel each other out. However, for masses above $2m_{K^+}$ but below $2m_{K^0}$, the left-hand loop is on the mass shell and is not strongly cancelled by the right-hand loop, which is still off the mass shell. Thus, the mixing strength is strongly enhanced for the ∼8 MeV mass window between the K^+K^- and $K^0\bar{K}^0$ thresholds.

BESIII searched for evidence for $f_0(980) \to a_0(980)$ mixing in the process $J/\psi \to \phi f_0 \to \phi a_0^0 \to K^+K^-\eta\pi^0$ using the 225M event J/ψ data sample, and for evidence for $a_0(980) \to f_0(980)$ mixing in the process $\psi' \to \gamma\chi_{c1} \to \gamma\pi^0 a_0^0 \to \gamma\pi^0 f_0 \to \gamma\pi^0\pi^+\pi^-$ using the 110M event ψ' data sample [21]. The $\eta\pi^0$ invariant mass distribution from the $J/\psi \to \phi a_0$ search is shown in the left

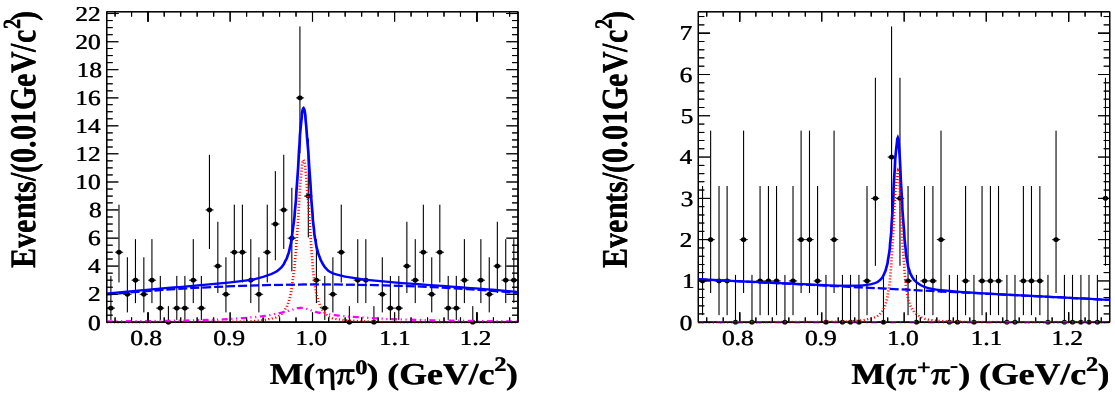

Figure 4: Left: The $\pi^0\eta$ mass distribution from $J/\psi \to \phi\pi^0\eta$ decays. **Right:** The $\pi^+\pi^-$ mass distribution from $\psi' \to \gamma\chi_{c1} \to \gamma\pi^0\pi^+\pi^-$ decays.

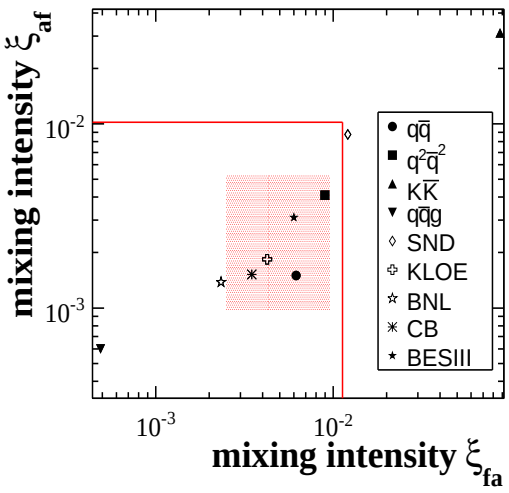

Figure 5: The shaded square indicates the $\pm 1\sigma$ ranges for the measured values of ξ_{fa} and ξ_{af} the $f_0 \to a_0$ and $a_0 \to f_0$ mixing probabilities, respectively. The solid red lines indicate 90% CL upper limits. The points represent expectations for different models and line-shape parameterizations (see Ref. [21]).

panel of Fig. 4, where a prominent narrow peak is seen at the expected location. The $\pi^+\pi^-$ mass distribution from the $\psi' \to \gamma\chi_{c1} \to \gamma\pi^0 f_0$ search is shown in the right panel of Fig. 4. Here some excess of events at the expected location can be seen.

From the fits shown as solid curves in the figures, BESIII determines probabilities for f_0 mixing to a_0^0, $\xi_{fa} = (0.60 \pm 0.34)\%$ or $< 1.1\%$ at the 90% confidence level (CL), and for a_0 mixing to f_0, $\xi_{af} = (0.31 \pm 0.21)\%$ or $< 1.0\%$ at the 90% CL.[4]

These limits imply that (ξ_{fa}, ξ_{af}) values outside of the box indicated by the solid red lines

[4]Here, and elsewhere in this report, statistical, systematic and model-dependence errors are added in quadrature.

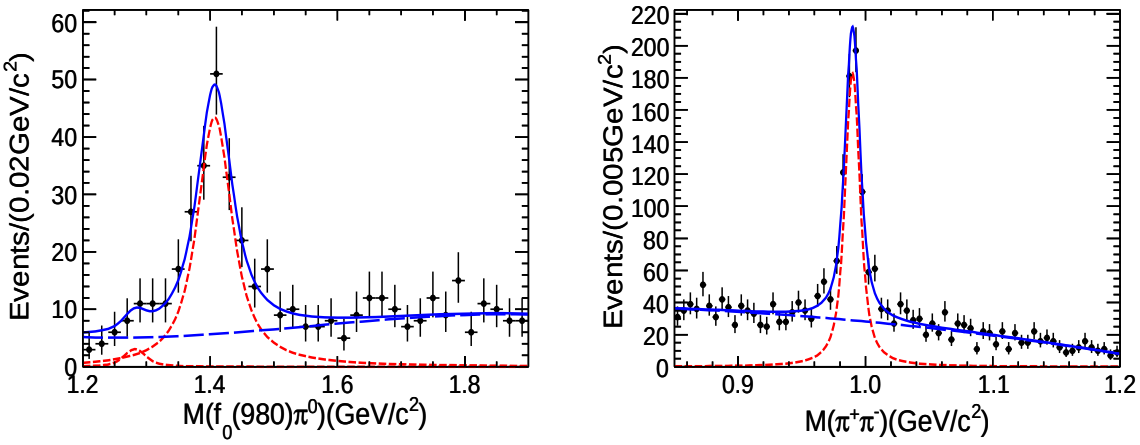

Figure 6: Left: The $\pi^0 f_0$ mass distribution from $J/\psi \to \gamma\pi^0 f_0$, decays where $f_0 \to \pi^0\pi^0$ (a $J/\psi \to 7\gamma$ final state!). **Right:** The $\pi^+\pi^-$ mass distribution from $\eta(1405) \to \pi^0 f_0$ decays where $f_0 \to \pi^+\pi^-$.

in Fig. 5 are ruled out; this includes the values expected for a pure $K\bar{K}$ molecule picture that are indicated in the figure by the solid triangular point near $(\xi_{fa}, \xi_{af}) = (0.1, 0.03)$.

2.3 Isospin violations in $\eta(1405)$ decays

In a separate study, BESIII examined the $\pi^0 f_0$ invariant mass distribution produced in radiative $J/\psi \to \gamma\pi^0 f_0$ decays for both the $f_0 \to \pi^+\pi^-$ and $f_0 \to \pi^0\pi^0$ decay modes [22]. In the distribution for $f_0 \to \pi^0\pi^0$ decays, shown in the left panel of Fig. 6 (the $f_0 \to \pi^+\pi^-$ channel looks similar), the dominant feature is a pronounced peak near $M(\pi^0 f_0) = 1405$ MeV; helicity analyses indicate that this peak has $J^p = 0^-$, which leads to its identification as the $\eta(1405)$ resonance.

The decay $\eta(1405) \to \pi^0 f_0$ violates isospin. In this case the observed isospin violation is quite large:

$$\frac{Bf(\eta(1405) \to \pi^0 f_0(980) \to \pi^0\pi^+\pi^-)}{Bf(\eta(1405) \to \pi^0 a_0(980) \to \pi^0\pi^0\eta)} = (17.9 \pm 4.2)\%, \tag{2.3}$$

which is an order-of-magnitude larger than is typical for isospin violations. (For example, BESIII also reports that the isospin violating $Bf(\eta' \to \pi^+\pi^-\pi^0)$ is $(0.9 \pm 0.1)\%$ of the isospin conserving $Bf(\eta' \to \pi^+\pi^-\eta)$ [22].)

A striking feature of these decays is the lineshape of the $f_0 \to \pi\pi$ decays, shown for the $f_0 \to \pi^+\pi^-$ channel in the right panel of Fig. 6, where it can be seen that the f_0 peak position is significantly above its nominal 980 MeV value, and its width is much narrower than its nominal value of $\sim$100 MeV. The fitted mass is $M = 989.9 \pm 0.4$ MeV, midway between $2m_{K^+}$ and $2m_{K^0}$, and the fitted width is $\Gamma = 9.5 \pm 1.1$ MeV, consistent with the $2m_{K^0} - 2m_{K^+} = 7.8$ MeV mass threshold difference.

Possible processes that mediate $\eta(1405) \to \pi^0 f_0$ are shown in Fig. 7. As we have seen above, the $a_0(980) \to f_0(980)$ process (Fig. 7a) is at or below the percent level, and is too small to account for the large isospin violation that is observed. Wu and collaborators [23] suggest that the triangle anomaly diagram shown in Fig. 7b could be large enough to account for the data. In this case, both

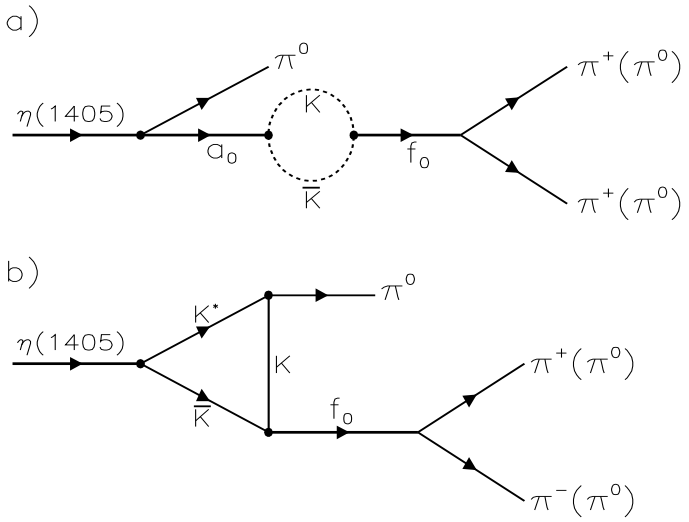

Figure 7: a) The leading diagram for $\eta(1405) \to \pi^0 f_0$ via $a_0(980)$-$f_0(980)$ mixing. **b)** The triangle anomaly diagram in $\eta(1405) \to \pi^0 f_0(980)$ decay [23].

the $K^*\bar{K}$ system that couples to the $\eta(1405)$ and the $K\bar{K}$ system coupling to the f_0 can have large on-mass-shell, isospin-violating contributions.

While our understanding of the low mass scalar mesons remains unclear, it seems that detailed studies – both theoretical and experimental – of isospin violations in processes involving the $a_0(980)$ and $f_0(980)$ can provide important probes of their inner workings. The results presented above are from data samples that are small fractions of what we ultimately expect to collect with BESIII. With the full data sets we will be able to provide theorists with precision measurements of the $a_0(980) \leftrightarrow f_0(980)$ mixing parameters and other quantities related to these mesons.

3. Some puzzles in J/ψ and ψ' decays

The charmonium mesons are (nearly) non-relativistic bound $c\bar{c}$ pairs and probably the simplest hadron system to understand. However, a number of puzzling features have been observed that seem to defy conventional understanding. I briefly mention a few of these here.

3.1 $\psi' \to \gamma\eta$ puzzle

The expected lowest-order diagram for $J/\psi \to \gamma\eta$ and $J/\psi \to \gamma\eta'$ is illustrated in Fig. 8a. If this diagram dominates, the ratio of partial widths for the two processes can be related to the η-η' mixing angle via the relation

$$\frac{\Gamma(J/\psi \to \gamma\eta)}{\Gamma(J/\psi \to \gamma\eta')} = (\frac{p_{\eta'}}{p_\eta})^3 \frac{1}{\tan^2\theta_P}, \tag{3.1}$$

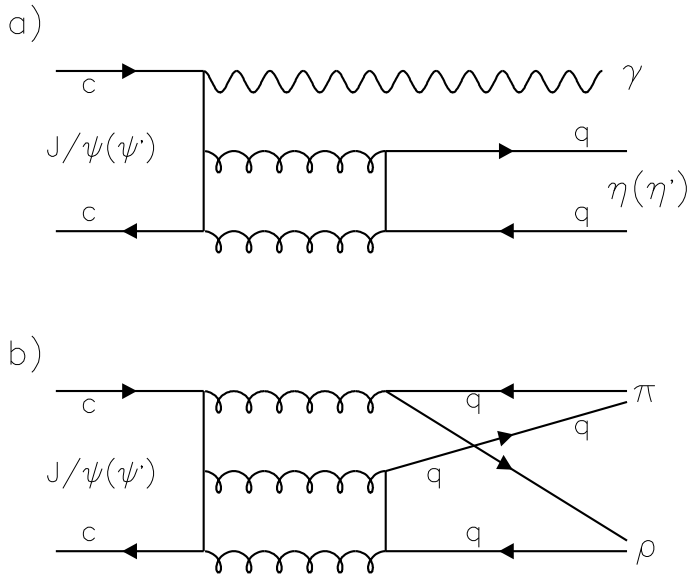

Figure 8: The lowest-order quark-line diagrams for **a)** $J/\psi\ (\psi') \to \gamma\eta\ (\eta')$ and **b)** $J/\psi\ (\psi') \to \rho\pi$.

where θ_P is the pseudoscalar mixing angle in the $SU(3)$ basis[5] and $(p_{\eta'}/p_\eta)^3$ is a phase-space factor [24]. From the PDG values for branching fractions, the ratio of partial widths is 0.21 ± 0.01, which gives $|\theta_P| = (22.5 \pm 0.5)^\circ$, consistent with the value determined from other methods.

The same diagram is expected to apply to $\psi' \to \gamma\eta$ and $\gamma\eta'$ decays in which case the same relation to the mixing angle should apply. However, although the mode $\psi' \to \gamma\eta'$ was well established long ago [25], only just recently did BESIII report [26] the first observation of a signal for $\psi' \to \gamma\eta$. For some unknown reason, the $\psi' \to \gamma\eta$ mode is strongly suppressed: the partial width ratio for the ψ' is only 0.011 ± 0.004, more than an order-of-magnitude lower than the corresponding ratio for the J/ψ. If this partial-width ratio is used in Eq. 3.1, the resulting value for $|\theta_P|$ is $(5.6 \pm 0.9)^\circ$, much smaller than the value determined from J/ψ decays.

3.2 The $\rho\pi$ puzzle: a new twist to an old story

The oldest puzzle in charmonium physics is the so-called $\rho\pi$ puzzle. $J/\psi \to \rho\pi$ is the strongest hadronic decay mode of the J/ψ, with a branching fraction of $(1.69 \pm 0.15)\%$ [15]. The lowest-order diagram for this decay is expected to be the three-gluon annihilation process shown in Fig. 8b. The same diagram is expected to apply to the ψ' and, thus, the partial width $\Gamma(\psi' \to \rho\pi)$ is expected to be that for the J/ψ, scaled by the ratio of the $c\bar{c}$ wavefunctions at the origin and

[5]This related to angle ϕ_P used in Eq. 2.2 by $\theta_P = \phi_P - \arctan\sqrt{2} = \phi_P - 54.7^\circ$.

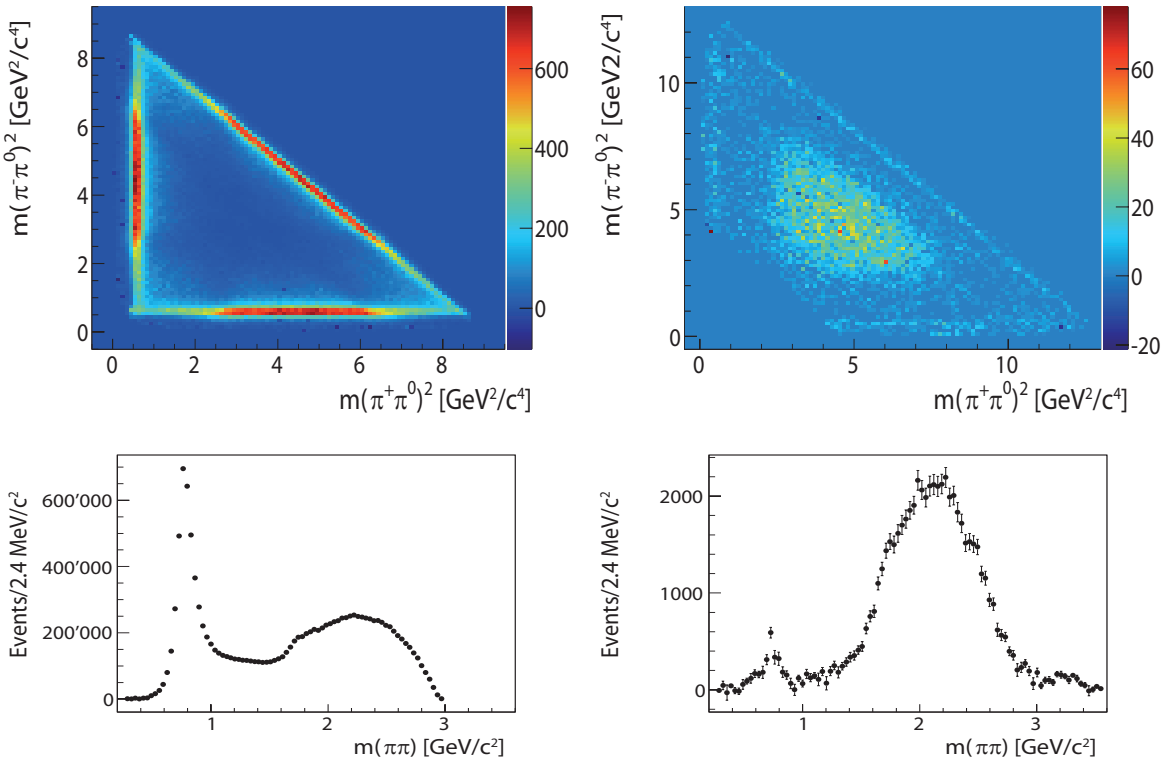

Figure 9: Top: the $M^2(\pi^-\pi^0)$ (vertical) *vs.* $M^2(\pi^+\pi^0)$ (horizontal) for (left) $J/\psi \to \pi^+\pi^-\pi^0$ and (right) $\psi' \to \pi^+\pi^-\pi^0$ decays. **Bottom:** the $M(\pi\pi)$ projections of the Dalitz plots.

a phase-space factor. (The ratio of the wavefunctions at the origin is determined by comparing the $J/\psi \to e^+e^-$ and $\psi' \to e^+e^-$ partial widths.) The result of this reasoning is the famous "12% rule," which says that the branching fraction for ψ' to some hadronic state should be (roughly) 12% that of the J/ψ to the same final state. While this simple rule more-or-less works for many decay modes, it fails miserably for $\psi' \to \rho\pi$ decays, where $Bf(\psi' \to \rho\pi) = (3.2 \pm 1.2) \times 10^{-5}$, nearly a factor of a hundred below the 12%-rule expectation.

BESIII has recently reported on a high-statistics study of of $J/\psi \to \pi^+\pi^-\pi^0$ and $\psi' \to \pi^+\pi^-\pi^0$ [27] using the 225M event J/ψ and 106M event ψ' data samples. The $M^2(\pi^-\pi^0)$ (vertical) *vs.* $M^2(\pi^+\pi^0)$ (horizontal) Dalitz plot distributions, shown in the top panels of Fig. 9, for the J/ψ (left) and ψ' (right) data samples, could not be more different. The center of the $J/\psi \to \pi^+\pi^-\pi^0$ Dalitz plot is completely devoid of events, while in the $\psi' \to \pi^+\pi^-\pi^0$ plot most of the events are concentrated in the center. The dynamics of the two processes are completely different, in spite of the fact that the underlying process –illustrated in Fig. 8b– is expected to be very similar. The $\rho\pi$ puzzle is becoming even more puzzling.

3.3 The subthreshold $p\bar{p}$ resonance seen in $J/\psi \to \gamma p\bar{p}$

As mentioned above in the introduction, BESII reported a peculiar mass-threshold enhancement in the $p\bar{p}$ invariant mass distribution in radiative $J/\psi \to \gamma p\bar{p}$ decays [7]. The shape of this

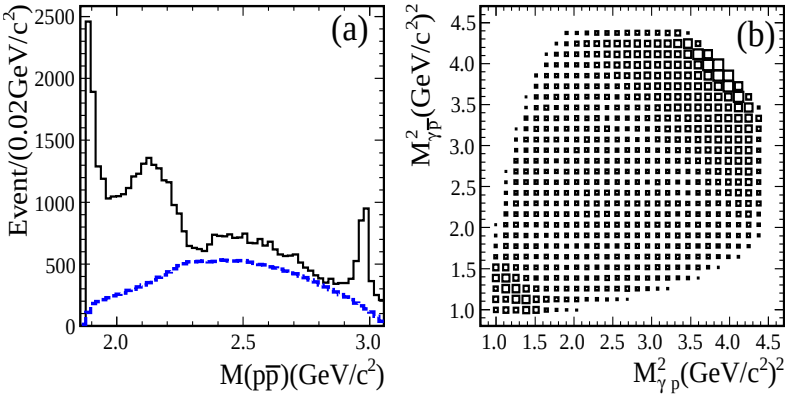

Figure 10: a) The $M(p\bar{p})$ distribution from $J/\psi \to \gamma p\bar{p}$ decays. The dashed curve is background from $J/\psi \to \pi^0 p\bar{p}$, where one of the photons from the $\pi^0 \to \gamma\gamma$ decay has low energy and is undetected. The narrow peak on the right is from $J/\psi \to \gamma\eta_c$, $\eta_c \to p\bar{p}$. **b)** The $M^2(\gamma\bar{p})$ (vertical) *vs.* $M^2(\gamma p)$ Dalitz plot for the same data sample. The diagonal band at the upper right is produced by the $p\bar{p}$ mass-threshold enhancement; the band at the lower left is due to the η_c.

low-mass peak cannot be reproduced by any of the commonly used parameterizations for final state interactions (FSI) between the final-state p and $\bar{p}$.

The $p\bar{p}$ invariant mass distribution for $J/\psi \to \gamma p\bar{p}$ decays in the 225M event BESIII J/ψ data sample is shown in Fig. 10a, where the threshold enhancement is quite prominent [28]. A Dalitz plot for these events is shown in Fig. 10b. A partial-wave-analysis (PWA) applied to these data determined that the J^{PC} of the near-threshold structure is 0^{-+}. A fit using a sub-threshold resonance shape modified by the Julich FSI effects [29] yields a mass of $M = 1832^{+32}_{-26}$ MeV and a 90% CL upper limit on the width of $\Gamma < 79$ MeV.

One intriguing theoretical speculation about this state is that it is a nucleon-antinucleon bound state, sometimes called baryonium. In this context some authors suggested that it may also decay to $\pi^+\pi^-\eta'$ at a substantial rate [30]. A BESII search for a corresponding state in $J/\psi \to \gamma\pi^+\pi^-\eta'$ decays found a previously unseen resonance, dubbed the $X(1835)$, with peak-mass value of 1834 ± 7 MeV and with a width of $\Gamma = 68 \pm 22$ MeV [31], both of which are in good correspondence with the fitted parameters of the $p\bar{p}$ subthreshold resonance peak and in accord with the prediction of Ref. [30].

Recently reported BESIII measurements of the $\pi^+\pi^-\eta'$ mass spectrum in $J/\psi \to \gamma\pi^+\pi^-\eta'$ are shown in the left panel of Fig. 11, where a peak corresponding to the $X(1835)$ is evident [32]. While the fitted value for the peak mass, $M = 1837^{+6}_{-4}$ MeV, is consistent with the BESII results for both the $\pi^+\pi^-\eta'$ and $p\bar{p}$ final states, the new results for the width are much larger, $\Gamma = 190 \pm 39$ MeV. The angular distribution of the radiated γ, shown in the right panel of Fig. 11, is consistent the $1+\cos^2\theta_\gamma$ form expected for $J^{PC} = 0^{-+}$. Although the mass and J^{PC} values are consistent with those in the $p\bar{p}$ channel, the broad width is not. However, the width determination of the $p\bar{p}$ peak has complications because of its sub-threshold character –we only see a small part of its high mass tail– while the $X(1835) \to \pi^+\pi^-\eta'$ peak has a large underlying background of real $\pi^+\pi^-\eta'$ events that likely has components that interfere with the $X(1835)$ resonance amplitude, a possibility that

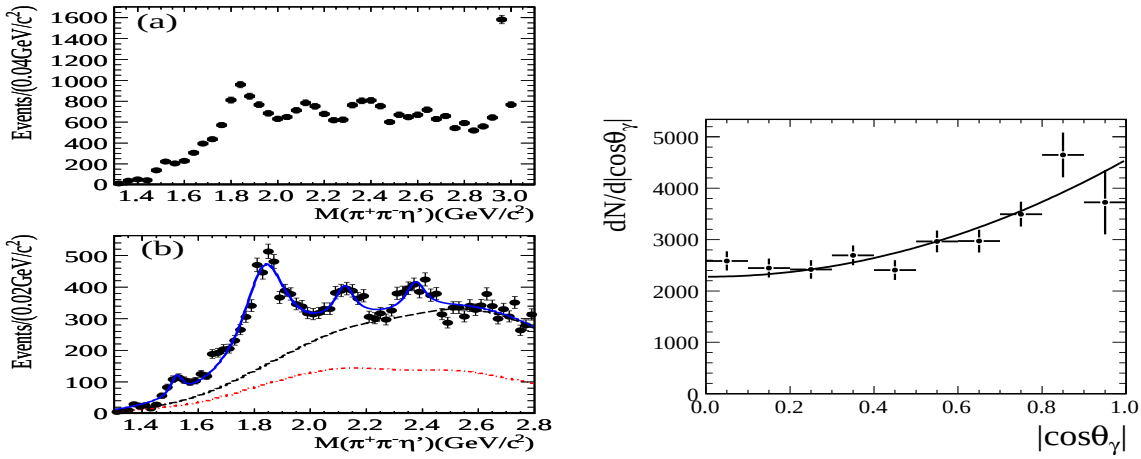

Figure 11: Left: The $\pi^+\pi^-\eta'$ mass distribution from $\psi' \to \gamma\pi^+\pi^-\eta'$. The red dash-dot curve in the bottom panel indicates the non-η' background determined from the η' mass side-bands. **Right:** The $X(1835)$ event yield in bins of $|\cos\theta_\gamma|$, where θ_γ is the polar angle of the angle of the radiated photon.

is not considered in the Ref. [32] fit for the $X(1835)$ mass and width.

An unexpected feature in the Fig. 11 (left) spectrum is the existence of two additional, rather pronounced peaks at higher masses. Fitted values for the masses and widths of these peaks are

$$M_1 = 2122^{+8}_{-7}\ \text{MeV}; \quad \Gamma_1 = 83^{+35}_{-19}\ \text{MeV} \tag{3.2}$$

$$M_2 = 2376^{+9}_{-10}\ \text{MeV}; \quad \Gamma_2 = 83^{+47}_{-18}\ \text{MeV}. \tag{3.3}$$

A striking characteristic of these peaks is their relatively narrow widths. Ordinary light-hadron resonances that are so far above threshold are expected to be very wide; there is no previously established light-hadron meson resonance with a width this narrow and a mass above 2 GeV. An intriguing possibility is that these states may be the 2^{++} and 0^{-+} glueballs for which an unquenched lattice QCD calculation predicts masses of 2390 ± 125 MeV and 2560 ± 125 MeV, respectively [33]. With the huge additional J/ψ event sample expected from future BESIII running, PWA will be used to determine the J^{PC} values of these peaks, which may help clarify their underlying nature.

4. Precise measurements of properties of the η_c and h_c charmonium states

The charmonium mesons are important because of their simplicity and their accessibility by a variety of theoretical approaches, including effective field theories and lattice QCD [34]. Because of their large mass, the charmed quarks bound in the charmonium meson states have relatively low velocities, $v^2 \sim 0.3$, and non-relativistic potential models can be used with relativisitic effects treated as small perturbations. With the discovery of the η_c' by Belle in 2002 [35] and the h_c by CLEO in 2005 [36], all of the charmonium states below the $M = 2m_D$ open-charm threshold have been identified (see Fig. 12). An experimental task now is the provision of precision measurements that can challenge the various theories that address this system. In this report I discuss recent BESIII measurements of properties the η_c and h_c charmonium states.

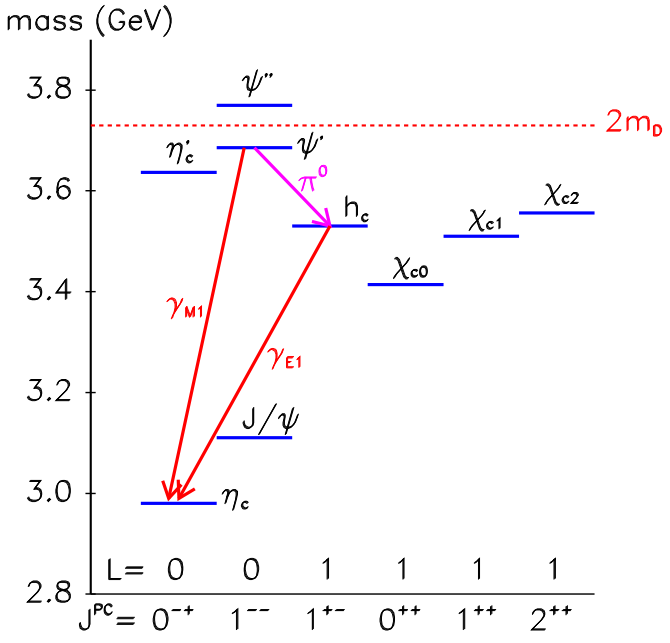

Figure 12: The spectrum of the low-lying charmonium mesons. The red dashed line indicates the $M = 2m_D$ open-charmed threshold. States with mass above this value can decay to final states containing D and $\bar{D}$ mesons and are typically broad; states below this threshold are relatively narrow. The magenta and red arrows indicate transitions used for the η_c and h_c measurements reported here.

4.1 Meaurement of the η_c mass and width

The η_c is the ground state of the charmonium system. The mass difference between the J/ψ and the η_c is due to hyperfine spin-spin interactions and is, therefore, a quantity of fundamental interest. However, while the mass of the J/ψ is known to very high precision –better than 4 PPM– the η_c mass remains poorly measured, the 2010 PDG world average (WA) value is $m_{\eta_c}^{2010} = 2980.3 \pm 1.2$ MeV, and the measurements that go into this average have poor internal consistency: the CL of the fit to a single mass is only 0.0018. The J/ψ-η_c hyperfine mass splitting derived from this WA is $\delta_{hfs} = 116.6 \pm 1.2$ MeV, a value that has always been above theoretical predictions [37]. The η_c width is also very poorly known; the 2010 PDG WA for this, $\Gamma_{\eta_c}^{2010} = 28.6 \pm 2.2$ MeV, has a confidence level of only 0.0001.

Measurements of the η_c mass and width roughly fall into two categories, depending on how the η_c mesons used in the measurement are produced. Experiments using η_c mesons produced via J/ψ radiative transitions tend to find a low mass (~ 2978 MeV) and narrow width (~ 10 MeV), while measurements using η_c mesons produced via two-photon collisions or B-meson decays find higher mass and width values. A primary early goal of the BESIII experiment has been to try to clear up this situation.

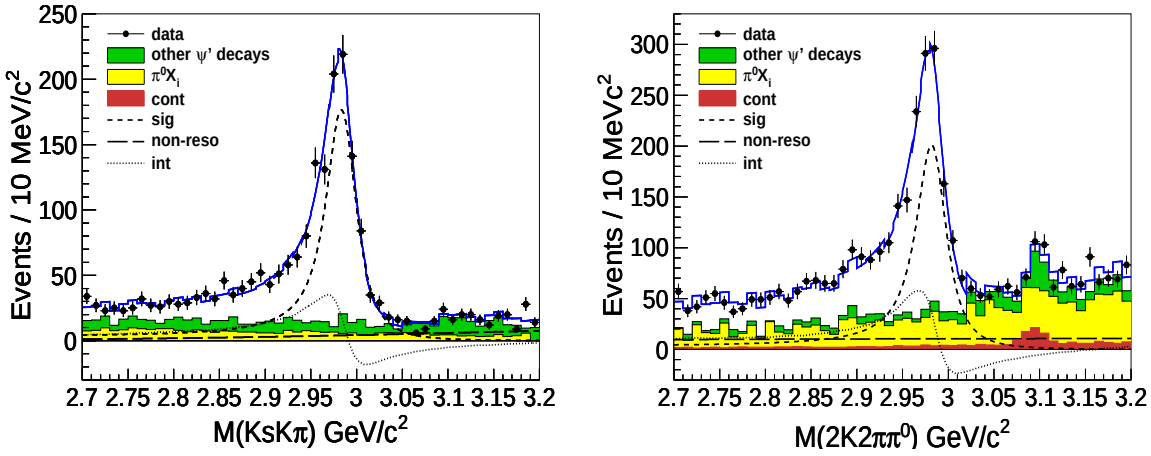

Figure 13: Left: The $K_SK^+\pi^-$ mass spectrum from $\psi' \to \gamma K_SK^+\pi-$ decays. **Right:** The corresponding plot for the $K^+K^-\pi^+\pi^-\pi^0$ channel. The main background in most channels, indicated as yellow histograms, are from $\psi' \to \pi^0 X_i$, where X_i is the same final state as the η_c decay mode that is under study, and the $\pi^0 \to \gamma\gamma$ decay is asymmetric where one γ has very low energy and is not detected. This background is incoherent and does not interfere with the η_c signal.

A recently reported BESIII mass and width measurement [38] uses samples of η_c mesons produced via the M1 radiative transition $\psi' \to \gamma\eta_c$ (indicated by a red arrow in in Fig. 12) that decay to one of six fully reconstructed final states:[6] $\eta_c \to X_i$, where $X_i = K_SK^+\pi^-$, $K^+K^-\pi^0$, $\eta\pi^+\pi^-$, $K_SK^+\pi^+\pi^-\pi^-$, $K^+K^-\pi^+\pi^-\pi^0$, and $3(\pi^+\pi^-)$, where $K_S \to \pi^+\pi^-$ and π^0 $(\eta) \to \gamma\gamma$. Distinct η_c signals are seen in each of the six channels, two typical mass spectra are shown in Fig. 13.

In all six channels, the η_c signal has a distinctively asymmetric shape with a long tail at low masses and a rapid drop on the high mass side. This is suggestive of possible interference with a coherent non-resonant background. The solid blue curves in Fig. 12 show the results of a fit that uses a Breit Wigner (BW) amplitude to represent the η_c that is weighted by a factor of E_γ^7 that accounts for the M1 transition matrix element (E_γ^3) and the wave-function mismatch between the radially excited ψ' and the ground-state η_c (E_γ^4); the fit also allows for interference with background from nonresonant $\psi' \to \gamma X_i$ decays. Since fits to individual channels give consistent results for the mass, width and the same value for the interference phase, a global fit to all six channels at once with a single mass, width and phase is used to determine the final results:

$$m_{\eta_c} = 2984.3 \pm 0.8 \text{ MeV} \tag{4.1}$$

$$\Gamma_{\eta_c} = 32.0 \pm 1.6 \text{ MeV}. \tag{4.2}$$

The value of the phase ϕ depends upon whether the constructive or destructive interference solution is used: $\phi_{cons} = 2.40 \pm 0.11$ or $\phi_{des} = 4.19 \pm 0.09$. (The mass and width values for the two cases are identical.) The reason that the interference phase is the same for all six channels is not understood.

The new BESIII mass and width values agree well with the earlier higher values found in two-photon and B-meson decay meaurements. The probable reasons for the low values found by

[6] The inclusion of charge conjugate states is implied.

earlier measurements using η_c mesons produced via radiative charmonium decays are the effects of the wave-function mismatch [39] and interference with the non-resonant background that were not considered. Using only the new BESIII η_c mass value, the J/ψ-η_c hyperfine mass splitting becomes smaller: $\delta_{hfs} = 112.6 \pm 0.8$ MeV, and in better agreement with theory.

4.2 Meaurements of h_c mass, width and branching fractions

The singlet P-wave h_c meson is notoriously difficult to study. In fact, despite considerable experimental efforts, it evaded detection for some thirty years until it was finally seen by CLEO in 2005 in the isospin-violating $\psi' \to \pi^0 h_c$ transition (indicated by a magenta arrow in Fig. 12) [36]. To date, it has only been seen by two groups, CLEO and BESIII [40] and only via the strongly suppressed $\psi' \to \pi^0 h_c$ process.

In lowest-order perturbation theory, the h_c mass is equal to the spin-weighted-average of the triplet P-wave $\chi_{c0,1,2}$ states: $< m_{\chi_{cJ}} >= (m_{\chi_{c0}} + 3m_{\chi_{c1}} + 5m_{\chi_{c2}})/9 = 3525.30 \pm 0.04$ MeV. Theoretical predictions for the branching fraction for $\psi' \to \pi^0 h_c$ are in the range $(0.4 \sim 1.3) \times 10^{-3}$, the E1 radiative transition $h_c \to \gamma\eta_c$ is expected to be the dominant decay mode with a branching fraction somewhere between $40 \sim 90\%$, and the h_c total width is expected to be less than 1 MeV [41].

Three detection & analysis methods have been used to study h_c production and decay, all of them use the processes indicated by arrows in Fig. 12:

inclusive In the "inclusive" mode, only the π^0 is detected and the h_c shows up as a peak in the mass recoiling against the detected π^0, which is inferred from conservation of energy and momentum. The inclusive mode signal yield is proportional the $Bf(\psi' \to \pi^0 h_c)$. This mode has the highest background.

E1-tagged In the "E1-tagged" mode the π^0 and the E1 transition γ from the $h_c \to \gamma\eta_c$, with energy in the range $465 - 535$ MeV, are detected. The E1-tagged signal yield is proportional to the branching fraction product $Bf(\psi' \to \gamma h_c) \times Bf(h_c \to \gamma\eta_c)$. The background for this mode is relatively smaller than that for the inclusive mode.

exclusive In the "exclusive" mode, the π^0, E1-γ and all of the decay products of the η_c are detected. Here all final-state particles are detected and energy-momentum conserving kinematic fits can be used to improve the resolution. The backgrounds are small and the yield is proportional to a triple product of branching fractions, including that for the η_c decay channel that is detected.

The CLEO observation used both the E1-tagged and exclusive modes. BESII has reported results from the inclusive and E1-tagged modes; an exhaustive study of exclusive channels is in progress.

The BESIII π^0 recoil mass distributions for the E1-tagged and inclusive modes are shown in Fig. 14. The E1-tagged sample (top) has the most distinct signal and this is used to determine the mass and width of the h_c. The solid curve in the figure is the result of a fit using a BW function convolved with a MC-determined resolution function to represent the signal, and a background shape that is determined from events with no photon in the E1 signal region, but with a photon in the E1-tag sidebands. From the fit, the mass and width are determined to be

$$m_{h_c} = 3525.40 \pm 0.22 \text{ MeV} \tag{4.3}$$

$$\Gamma_{h_c} = 0.73 \pm 0.53 \text{ MeV}; \tag{4.4}$$

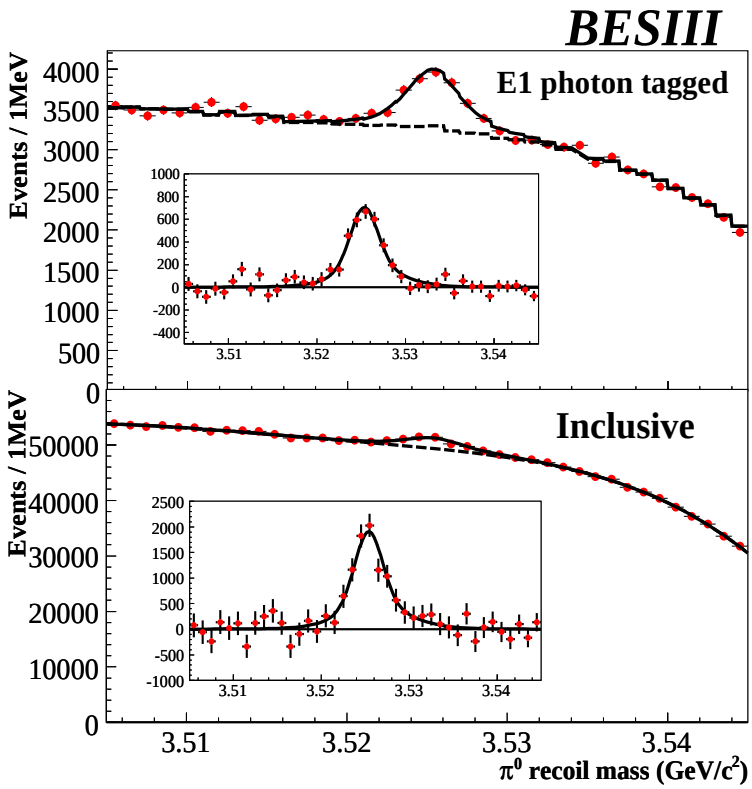

Figure 14: The π^0 recoil mass for E1-tagged (top) and inclusive (bottom)$\psi' \to \pi^0 X$ decays. The insets show the signal yields with the fitted backgrounds subtracted.

the 90% CL upper limit on the width is $\Gamma_{h_c} < 1.44$ MeV. With this mass value, the P-wave hyperfine splitting is $< m_{\chi_{cJ}} > - m_{h_c} = -0.10 \pm 0.22$ MeV, consistent with zero. From the signal yield, the product branching fraction $Bf(\psi' \to \pi^0 h_c) \times Bf(h_c \to \gamma\eta_c) = (4.48 \pm 0.64) \times 10^{-4}$ is determined.

The inclusive π^0 recoil mass distribution is shown in the lower part of Fig. 14. Here the solid curve is the result of a fit where the mass and width of the signal function are fixed at the E1-tagged results and the background is parameterized by a fourth-order Chebyshev polynomial with all parameters allowed to float. The signal yield and the product branching fraction results from the E1-tagged mode are used to make the first determination of the individual branching fractions:

$$Bf(\psi' \to \pi^0 h_c) = (8.4 \pm 1.6) \times 10^{-4} \quad (4.5)$$

$$Bf(h_c \to \gamma\eta_c) = (54.3 \pm 8.5)\%, \quad (4.6)$$

which are within the range of theoretical expectations.

5. Other BESIII activities

The results described in this report correspond to only a small fraction of the total BESIII physics activity. A more complete overview of the entire physics program planned for BESIII is provided in an 800 page tome published in 2009 [42].

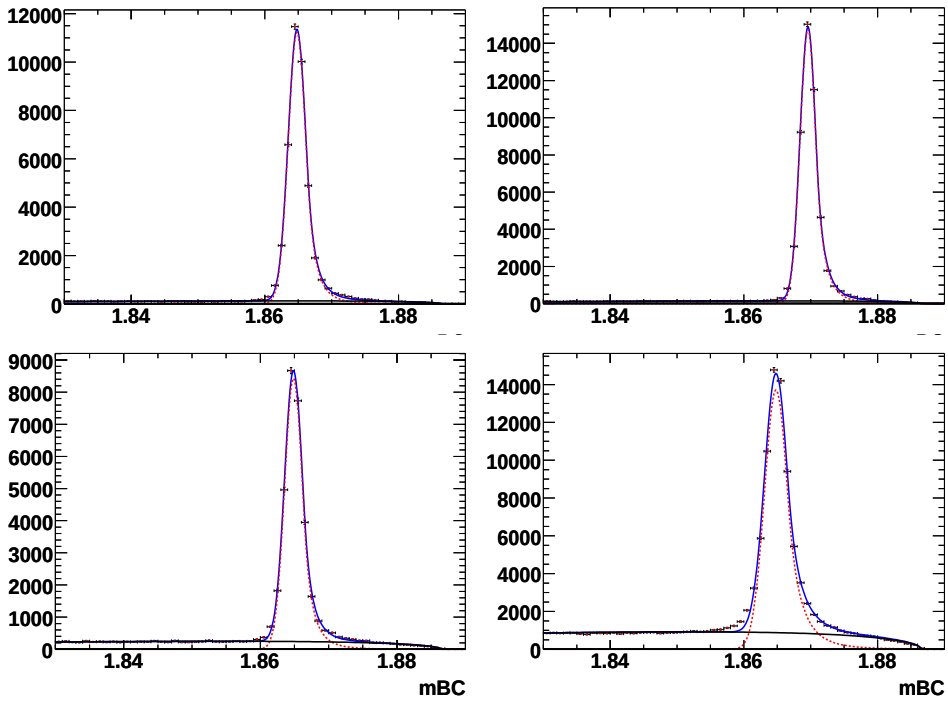

Figure 15: Reconstructed D-meson mass distributions for **top:** $D^0 \to K^-\pi^+$ (left) & $D^+ \to K^-\pi^+\pi^+$ (right), and **bottom:** $D^0 \to K^-\pi^+\pi^+\pi^-$ (left) & $D^0 \to K^-\pi^+\pi^0$ (right). The horizonal axis units are GeV.

5.1 Charmed meson physics

The most notable subject that I have skipped in this report is the BESIII charmed physics program that is aimed primarily at precision studies of weak decay processes of D and D_s mesons. The initial phase of this program was a long data-taking run that accumulated 2.9 fb^{-1} at the peak of the $\psi(3770)$ charmonium meson. This is a resonance in the $e^+e^- \to D\bar{D}$ channel with a peak cross section of about 6 nb at a c.m. energy that is about 40 MeV above the $E_{c.m.} = 2m_D$ open-charm mass threshold. (The $\psi(3770)$ is included in the sketch of the charmonium spectrum shown in Fig. 12.) At least 90%, maybe more, of $\psi(3770)$ decays are to $D\bar{D}$ meson pairs and nothing else; there is not enough enough c.m. energy to produce any other accompanying hadrons. As a result, The energy of each D meson is half of the total c.m. energy, which is precisely known. Thus, when a D meson is reconstructed in an event, the recoil system is "tagged" as a $\bar{D}$, and the constraint on the energy results in reconstructed D-meson mass signals that have excellent resolution ($\sigma = 1.3$ MeV for all charged modes and $\sigma = 1.9$ MeV for modes with one π^0) and signal to noise. D-meson signals for four commonly used tag decay modes are shown in Fig. 15. Moreover, the $D\bar{D}$ system is in a coherent, P-wave quantum state with $J^{PC} = 1^{--}$. This coherence is unique to D mesons originating from $\psi(3770) \to D\bar{D}$ decays and permits a number of interesting measurements [43]. For example, if one D meson is tagged in a pure CP decay mode (such as K^+K^-, $\pi^+\pi^-$ or $K_S\pi^0\pi^0$ for $CP = +1$, and $K_S\pi^0$, $K_S\eta$ or $K_S\omega$ for $CP = -1$), the decay of the accompanying D meson to a CP eigenstate with the same CP eigenvalue would be an unambiguous signal for CP violation.

The 2.9 fb^{-1} data sample that has already been collected contains almost 20M $D\bar{D}$ meson pairs and is about three times the world's previous previously largest $\psi(3770)$ event sample –collected

by CLEOc– and is currently being used for numerous analyses aimed at searches for rare decays & new physics, and improving on the precision of previous measurements. In many of the latter cases, the measurements are of form-factors that are accessible in lattice QCD calculations. As the precision of lattice QCD improves, BESIII will provide more precise measurements that continue to challenge the theory.

Ultimately, over the next seven years or so, BESIII intends to collect a total of ~ 10 fb^{-1} at the $\psi(3770)$ for D meson measurements and a comparable sample at higher energy for D_s meson studies.

5.2 Additional J/ψ and ψ' data samples.

The results reported above are based on 106M event ψ' and 225M event J/ψ data samples. The ultimate goal of the BESIII program is to collect a total of $\sim 10^9$ ψ' events and a multiple of 10^9 J/ψ events. These samples will be used, among other things, for detailed PWA of the many unassigned resonance peaks that have been seen, studies of baryon spectroscopy, and high-statistics measurements of isospin-violating processes that are proving to be valuable probes of the structure of near-threshold resonances. In addition, with the huge J/ψ data sample, the expected SM level for weak decays of the J/ψ to final states containing a single D or D_s meson can be accessed and searches for non-SM weak decays and lepton-flavor-violating decays, such as $J/\psi \to e^+\mu^-$, will have interesting sensitivity.

5.3 QCD, two-photon, τ and XYZ-meson physics

BESIII also plans to redo the total cross section measurements for $e^+e^- \to$ *hadrons* with higher precision over the entire accessible c.m. energy range, measure π^0 and η formfactors in two-photon collisions, remeasure the τ mass with much improved accuracy, and do studies of the recently discovered XYZ mesons.

Cross section measurement scans will cover c.m. energies from near the nucleon-antinucleon threshold up to the $\Lambda_c^+\Lambda_c^-$ threshold. The data near the nucleon-antinucleon threshold will be used to measure neutron form factors [44].

The τ mass measurement will benefit from a high-precision beam-energy monitor based on the detection of Compton scattering of back-scattered photons from a high powered single-mode infrared laser. This system has been commissioned and routinely measures the beam energy with a precision of $\delta_{E_{\rm beam}}/E_{\rm beam} \simeq 10^{-5}$ [45].

Data taken in a dedicated run at $E_{c.m.} \simeq 4260$ MeV will be used to study $Y(4260)$ decays. Sensitive searches for possible new, exotic mesons that decay to $\pi^+ J/\psi$ and $\pi^+ h_c$, analogous to the $Z_1(10610)^+$ and $Z_2(10650)^+$ mesons seen by Belle in the $b\bar{b}$ bottomonium meson system [46], will be performed for $\pi^+\pi^- J/\psi$ and $\pi^+\pi^- h_c$ final states.

6. Concluding remarks

The BESIII experiment at the Institute of High Energy Physics in Beijing, China is up and running and producing interesting results on a variety fo topics. The BEPCII collider is performing near design levels and the BESIII detector performance is excellent. We expect to produce many interesting new results in the coming decade.

7. Aknowledgements

I thank the meeting organizers for inviting me to report on BESIII results at this interesting and well organized meeting. I also thank my BESIII colleagues for allowing me to represent them and for generating the results discussed herein. I benefited from an informative conversation with Qiang Zhao; Nik Berger, Liaoyuan Dong & Yadi Wang provided me with some of the figures used in this report; and Haibo Li provided a number of suggestions and corrections. This work was supported by the National Research Foundation of Korea under WCU-program Contract No. R32-2008-000-10155-0 and Grant No. 2011-0029457.

References

[1] J.Z. Bai *et al.* (BES Collaboration), Phys. Rev. Lett. **69**, 3021 (1992).

[2] J.Z. Bai *et al.* (BES Collaboration), Phys. Rev. Lett. **84**, 594 (2000).

[3] H. Burkhardt and B. Pietrzyk, Phys. Lett. **B513**, 46 (2001).

[4] J.Z. Bai *et al.* (BESII Collaboration), Phys. Rev. Lett. **88**, 101802 (2002).

[5] M. Ablikim *et al.* (BESII Collaboration), Phys. Lett. **B633**, 681 (2006).

[6] M. Ablikim *et al.* (BESII Collaboration), Phys. Lett. **B598**, 149 (2004).

[7] J.Z. Bai *et al.* (BESII Collaboration), Phys. Rev. Lett. **91**, 022001 (2003).

[8] M. Gell-Mann, Phys. Lett. **8**, 214 (1964).

[9] G. Zweig, CERN Report 8419/Th.401 (1964), *An SU_3 Model For Strong Interaction Symmetry and its Breaking*.

[10] W.-M. Yao *et al.* (Particle Data Group), J. Phys. G: Nucl. Part. Phys. **33** (2006), 1. See, in particular "Pentaquark Update" by G. Trilling on page 1019; see also the review by R. A. Schumacher, arXiv:nucl-ex/051204.

[11] See, for example, V. Dorofeev (VES Collaboration) hep-ex/9905002 and G.S. Abrams *et al.* (E852 Collaboration), Phys. Rev. Lett. **81** (1998), 5760.

[12] See, for example, T. Barnes, arXiv:hep-ph/0007296.

[13] A. Bramon, R. Escribano and M.D. Scadron, Phys. Lett. **B503**, 271 (2001).

[14] For a quantiative relation between the mixing angle and meson masses, one needs to use the Gell-Mann-Okubo mass relations: S. Okubo, Prog. Theor. Phys. 27 (1962), M. Gell-mann, *The Eightfold Way, A Theory of Strong Interaction Symmetry*, Caltech Report CTSL-20 (1961), unpublished.

[15] Unless otherwise noted, numbers given in this report are taken from K. Nakamura, *et al.* (Particle Data Group), Jour. Phys. G **37**, 075021 (2010).

[16] M. Ablikim *et al.* (BESII Collaboration), Phys. Lett. **B607**, 243 (2005).

[17] A. Abele *et al.* (Crystal Barrel Collaboration), Phys. Rev. D **57**, 3860 (1998).

[18] R.L. Jaffe, Phys. Rev. D **15**, 267 (1977).

[19] J.D. Weinstein and N. Isgur, Phys. Rev. D **27**, 588 (1983).

[20] C. Hanhart, B. Kubis and J.R. Pelaez, Phys. Rev. D **76**, 074028 (2007), see also J.J. Wu and B.S, Zou, Phys. Rev. D **7**8, 074017 (2007).

[21] M. Ablikim *et al.* (BESIII Collaboration), Phys. Rev. D **83**, 032003 (2011).

[22] M. Ablikim *et al.* (BESIII Collaboration), arXiv:1201.2737, to appear in Physical Review Letters.

[23] J.J. Wu, X.-H. Liu, Q. Zhao and B.S. Zou, Phys. Rev. Lett. **108**, 081803 (2012).

[24] R.M. Cahn and M.S. Chanowitz, Phys. Lett. **B59**, 277 (1975).

[25] J.Z. Bai *et al.* (BES Collaboration), Phys. Rev. D **58**, 097101 (1998).

[26] M. Ablikim *et al.* (BESIII Collaboration), Phys. Rev. Lett. **105**, 261801 (2011).

[27] M. Ablikim *et al.* (BESIII Collaboration), arXiv:1202.2048, submitted to Physical Letters B.

[28] M. Ablikim *et al.* (BESIII Collaboration), arXiv:1112.0942, to appear in Physical Review Letters; see also M. Ablikim *et al.* (BESIII Collaboration), Chin. Phys. C **34**, 421 (2010).

[29] E. Klempt, F. Bradamente, A. Martin and J.M. Richard, Phys. Rep. **368**, 119 (2002).

[30] G.J. Ding and M.L. Yan, Phys. Rev. C **72**, 045207 (2005).

[31] M. Ablikim *et al.* (BESII Collaboration), Phys. Rev. Lett. **95**, 262001 (2005).

[32] M. Ablikim *et al.* (BESIII Collaboration), Phys. Rev. Lett. **95**, 262001 (2005).

[33] Y. Chen *et al.*, Phys. Rev. D **73**, 014516 (2006).

[34] For a recent review see N. Brambilla *et al.*, Eur. Phys. J. C **71**, 1534 (2011).

[35] S.-K. Choi *et al.* (Belle Collaboration), Phys. Rev. Lett. **89**, 102001 (2002).

[36] J. Rosner *et al.* (CLEO Collaboration), Phys. Rev. Lett. **95**, 102003 (2005).

[37] See, for example, G. Bali *et al.*, PoS LATTICE2010, 134 (2011), arXiv:1011.2195 [hep-lat].

[38] M. Ablikim *et al.* (BESIII Collaboration), arXiv:1111.0398, submitted to Physical Review Letters.

[39] The importance of the wave function mismatch factor was first pointed out in R. Mitchell *et al.* (CLEO Collaboration), Phys. Rev. Lett. **102**, 011801 (2009).

[40] M. Ablikim *et al.* (BESIII Collaboration), Phys. Rev. Lett. **104**, 132002 (2010).

[41] Y.P. Kuang, S.F. Tuan and T.M. Yan Phys. Rev. D **37**, 1210 (1988), P. Ko, Phys. Rev. D **52**, 1710 (1995), Y.P. Kuang, Phys. Rev. D **65**, 094024 (2002), and S. Godfrey and J. Rosner, Phys. Rev. D **66**, 014012 (2002).

[42] D.M. Asner *et al.*, Int. J. Mod. Phys. A **24**, Supplement-1, 1 (2009).

[43] See, for example, D.M. Asner and W.M. Sun, Phys. Rev. D **73**, 034024 (2006).

[44] R. Baldini, S. Pacetti and A. Zallo, Nucl. Phys. Proc. Suppl. **219-220**, 32 (2011).

[45] E.V. Abakumova *et al.*, Nucl. Instrum. Meth. **A659**, 21 (2011).

[46] A. Bondar *et al.* (Belle Collaboration), arXiv:1110.2251, to appear in Physical Review Letters.